Reduction of the time and simulation calculations of detecting buried targets by using the airborne GPR antenna footprint

E. Shahroosvand[1] and M. Kazerooni[1*]
Faculty of Electrical & Computer Engineering, Malek Ashtar University of Technology, Iran
shahroosvandehsan@mut.ac.ir, kazerooni@mut.ac.ir
Corresponding author: kazerooni@mut.ac.ir

Abstract- In this paper, the calculation of the dimensions of the area illuminated by the antenna (antenna footprint) of an Airborne Ground Penetrating Radar (airborne GPR) has been investigated on the surface and the subsurface. In the topic of detecting buried targets by airborne GPR radars, knowing the area illuminated by the radar antenna is very important. The effective factors in determining the dimensions of the illuminated area on the surface are the position of the radar antenna, the azimuth and elevation half-power beam width, and on ground's the subsurface, in addition to the above-mentioned parameters, the relative permittivity of the ground and the height of the desired area to the ground's surface, the type of polarization and the refraction angle of the waves sent from the radar are dependent. By having the dimensions of the illuminated area, we can cell the search area according to it and excite these cells with appropriate power and at a certain time. The advantages of cell confinement according to the antenna footprint are managing the transmitted power and reducing the search time. Another advantage of using a radiation plane to the size of the antenna footprint is the detection of small targets that are close to each other. In this case, when the radiation port is placed above any target, that target will be revealed. In this paper, two methods are provided to simulate the detection of buried targets in CST software. In the first method, a horn antenna is used as a radiation element in the structure itself, but in the second method, the antenna is simulated separately and its parameters are used to calculate the antenna footprint. In the first method, the meshing is very large due to the distance between the antenna and the ground's surface, which increases the simulation time, but in the second method, due to the removal of this distance and the use of the antenna footprint as a radiation element, the meshing And the simulation time is greatly reduced.

Index Terms- Airborne GPR, antenna footprint, buried targets, reduction of mesh cells, search time.

I. INTRODUCTION

In today's era, detecting, identifying, and imaging the buried underground target is one of the most important challenges in the field of remote sensing [1, 2]. Scientists in this field try to succeed in this challenge by using all their technological capacities. Currently, the detection and identification of the buried target are carried out in four geophysical, optical, radar, and radiation fields[3]. Radar methods are one of the most widely used methods of detecting and identifying a buried target, which uses electromagnetic waves to detect and identify it. Among its most important methods, we can mention ground-penetrating radar (GPR), Synthetic aperture Ground penetrating radar (GPR-SAR), and Interferometry Synthetic Aperture Radar (InSAR) [4–7].

Among the radar methods, airborne GPRs have attracted the attention of scientists and experts in the field of detecting and identifying buried targets due to their high accuracy, simplicity in implementation, and ability to be used remotely. GPR simulation offers scientists and researchers a powerful tool for testing and evaluating radar performance, optimizing radar settings and parameters, and developing new and innovative approaches to GPR technology. Overall, using a target detection simulator in GPRs can provide a cost-effective, flexible, and reproducible way to test and evaluate the radar's performance, optimize its settings and parameters, and improve its detection and imaging capabilities. Reducing complexity and simulation time in GPRs can lead to increased efficiency, improved accuracy, and cost reduction. These benefits can help advance the development of GPR technology and improve its effectiveness in various applications. In recent years, CST software has been used in many articles to simulate the application of GPR radar, some of which are mentioned in this section.

Ch.K. Hailma and his colleagues[8] in their research discuss the method of processing the pulse modulation (PM) ground penetrating radar (GPR) system to detect an embedded object underground. They used the CST software for the simulation of the target detection by using a Dipole antenna as a GPR antenna to transmit the waves.

M. Razali and his colleagues[9] in their research for generating radargram images, data from the antenna output signal that has been simulated in a complete GPR system simulation model developed using CST software will be taken and exported into MATLAB software.

S. H. Dahlan and his colleagues[10] in their research, a GPR Hybrid system which is a mix of the AM GPR and the SFCW GPR was proposed, simulated, tested, and produced. The simulation results of the GPR Hybrid system emulating object detection showed accurate detection of the object in the CST software.

M .S .Sulong and his colleagues[11] in their research, a Horn antenna designed using the CST software for GPR antenna. The simulation results show that the output signal of the Horn antenna can be used in detecting embedded objects that are made from material of wood and iron.

In all the simulations of the above researches, the antenna used is above the soil the surface and

attached to the surface. In this case, the space of the simulation environment will have a balanced cell mesh. If the antenna is separated from the surface of the box and placed at a certain height (in airborne GPR applications), the space between the surface and the antenna will be meshed, which will greatly increase the number of mesh cells. Increasing the number of mesh cells will slow down the simulation process and make it more complicated. This article aims to reduce the number of mesh cells and simplify the simulation of detecting buried targets

II.   AIRBORNE GPR PRINCIPLE

The operating principle of GPR is based on the propagation and scattering of electromagnetic (EM) waves in matter, offering thus an alternative to nondestructive testing and evaluation (NDT & NDE) methods based on energy–matter interactions of mechanical waves such as ultrasound[12]. Therefore, instead of dealing with mechanical properties, GPR is based on the varying properties of EM constitutive parameters (permittivity ε, conductivity σ, and permeability μ) and their interaction with EM waves to locate, identify, and image embedded targets in host media[13]. The electromagnetic field emitted by the radar interacts with the investigated scenario: reflection, transmission, and scattering phenomena occur at any interface corresponding to a change in dielectric properties[14].

Ground-penetrating radar (GPR) provides high-resolution images of subsurface and structures through wide-band electromagnetic waves. It operates in a wide range of frequencies, from 10 MHz to 5 GHz for impulse systems and from 1 to 8 GHz for stepped-frequency systems[15]. From a high-level perspective, a GPR system primarily consists of a data collection unit, a transmitting unit, a receiving unit, and antenna units. The type and position of antennas and the size and shape of the structure under test determine the amount and quality of measurements[16]. Depending on the number and position of transmitting/receiving antennas, there are three possible operating modes: 1. monostatic, whereby a transmitting/receiving antenna is located at the same place over the material under test. 2. Bistatic, whereby transmitting and receiving antennas are at different positions. 3. Multistatic, whereby multiple transmitters and/or multiple receivers, usually designed to form antenna arrays, can be located at different positions[2].

GPR systems are either ground-coupled or air-coupled. In Ground-coupled GPR, antennas are placed directly on the ground surface and then dragged over it. In Airborne GPR, antennas are often mounted on a vehicle, aircraft, or Unmanned aerial vehicle (UAV) that drives or flies over the ground[17]. A typical monostatic airborne GPR scenario is shown in Fig. 1.

he GPR operation may be described in four broad steps. In the first step, EM waves from the transmitting antenna are directed into the host medium (ground). Then the second step, typical reflection–refraction phenomena occur at interfaces, whereby the scattered wave reflects part of the incident energy, and the remainder of energy travels through interfaces at a different velocity to
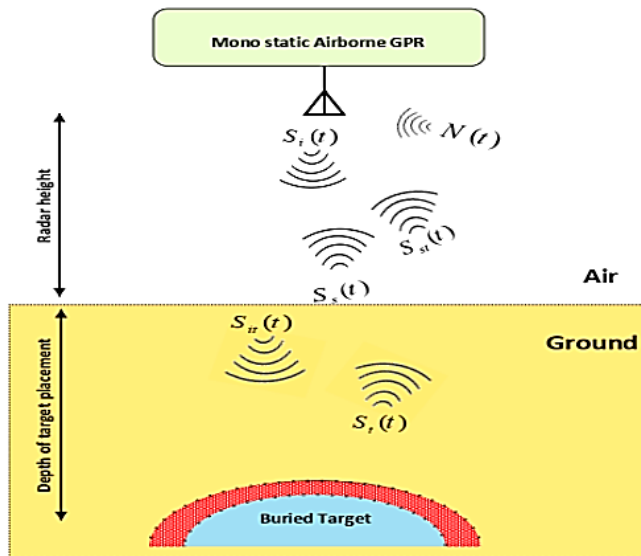
Fig. 1. The schematic of a typical monostatic airborne GPR

greater depths in the host. In the third step, the refracted waves propagate through the host medium reaching a boundary of different electrical characteristics (called flaw or target). Finally, at the fourth step, this scattered wave (also called echo) travels back from the target to the receiving antenna.

The physics of GPR is based on the reflection, refraction, and scattering processes that transform the incident wave into a received signal with an amplitude and phase different from the transmitted wave. The particular received waveform is determined primarily by the electrical contrast (i.e., ratios of relative permittivity and conductivity of targets and host media) as well as the particular dimensions and shape of targets[14].

In practical considerations of GPR, the depth of penetration and resolution are also directly related to the pulse waveform and its frequency content. Time-domain or pulsed radars, commonly used in practice, are based on the radiation of a particular waveform with a high bandwidth, which eases the identification of targets and flaws by the presence of scattered waves, in a process called time-windowing. On the other hand, frequency domain GPR systems use frequency modulation, whereby a carrier frequency scans bandwidths with a fixed step. Stepped-frequency continuous-wave (SFCW) systems are available in commercial GPRs, and their use is on the rise due to advantages over pulsed radars in terms of shaping the power spectral density and a higher mean power[14].

In summary, any GPR equipment has to be chosen according to the particular application (or class of applications) and the characteristics of the target and host media. This choice also involves a trade-off between resolution and penetration depth, both key factors for the success in the detection and classification of targets.
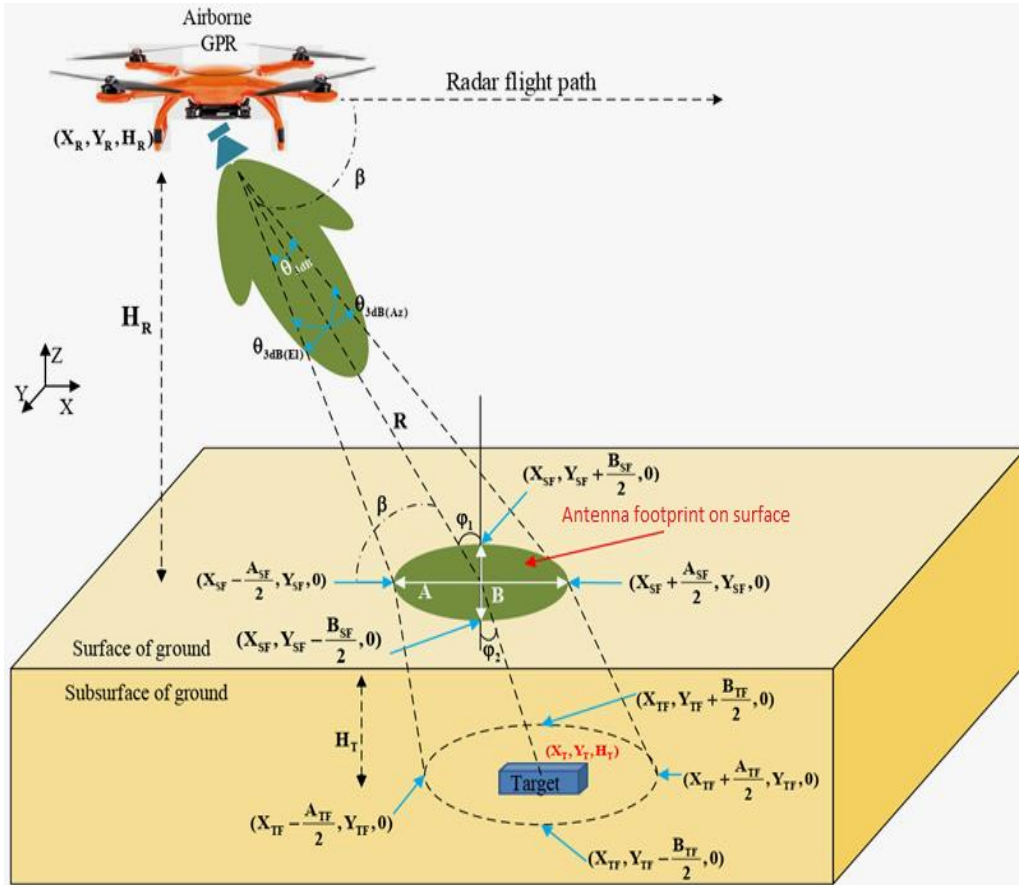
Fig. 2. The illuminated area by the antenna on the surface and subsurface

A. Antenna footprint

In radio and radar systems, the antenna is responsible for sending and receiving electromagnetic waves. The waves radiated by the transmitter antenna illuminate the range of the earth's surface, which is called the area illuminated by the antenna, the coverage area, or the antenna footprint. Fig 2 shows the illuminated area by the antenna. For normal incidence (Radar is in the vertical position and above ground), the transmission coefficient at a boundary between two media is independent of the polarization of the incident wave, as both the electric and magnetic fields of a normally incident plane wave are tangential to the boundary regardless of the wave polarization. This is not the case for obliquely incident waves traveling at an angle concerning the normal to the interface[18].

The plane of incidence is the plane containing the direction of wave travel and the surface normal to the boundary. A wave is perpendicularly polarized (also called horizontally polarized) when its electric field vector is perpendicular to the plane of incidence and parallel polarized (also called vertically polarized) when its electric field vector lies in the plane of incidence[18].

1) Antenna footprint in the oblique position

The cross-section of the environment illuminated by the radar antenna on the surface can be

circular, symmetric, or asymmetric ellipse[19]. The size of the cross-sectional area of the antenna footprint on the surface depends on several factors, including the height of the radar antenna(H_R), the angle of the antenna for the horizon(β), the azimuth half-power beam width ($\theta_{3dB(AZ)}$), and the elevation half-power beam width($\theta_{3dB(AZ)}$). The illuminated area in the ground's subsurface can be calculated by taking into account the refraction angle(φ_1) $\neq 0$, the electrical permittivity of the subsurface (ε_r), the beam shape factor(α) for a Gaussian beam = 1.33, and the depth of the illuminated surface to the ground level(H_T). Fig 2 shows the illuminated area by the antenna on the surface and subsurface in this case.

a)   Antenna footprint on the surface

The sizes of the cross-sectional area of the antenna footprint on the surface are given by equations (1-3). In these equations are the semi-major ax and the semi-minor of the elliptical illumination on the surface. is the illuminated surface area on the surface [19].

$$A_{SF(m)} = \frac{2H_R \sin\beta}{\alpha} \tan(\frac{\theta_{Az}}{2}) \tag{1}$$

$$B_{SF(m)} = \frac{2H_R}{\alpha} \tan(\frac{\theta_{El}}{2}) \tag{2}$$

$$S_{SF(m^2)} = \frac{\pi(2H_R)^2 \sin\beta}{\alpha^2} \tan(\frac{\theta_{Az}}{2}) \tan(\frac{\theta_{El}}{2}) \tag{3}$$

In the pulsed radars, if the pulse width is much shorter than the length of the elliptical footprint due to elevation beam width, In this case, the illuminated area is given by the area of a rectangle, one of whose sides is the length of the elliptical footprint in azimuth direction and the other is the pulse length measured along the surface in the elevation direction. The length of the elliptical footprint in the azimuth direction is given by equation (1). The pulse length measured along the surface is given by equation (4) and the illuminated area is given by equation (5).

$$PL_{(m)} = \frac{c\tau}{2} \sec\beta \tag{4}$$

$$S_{SF(m^2)} = \frac{\pi c\tau H_R}{\alpha} \tan(\frac{\theta_{Az}}{2}) \tan\beta \tag{5}$$

In the above equations, $c_{(m/s)}$ is the velocity of electromagnetic waves in free space and $\tau_{(S)}$ is radar transmitted pulse width[19]

b)   Antenna footprint in the subsurface

Electromagnetic waves during their propagation path after hitting the ground's surface, some of it

is reflected into the air and another amount of it enters the ground. Among the effective factors in the penetration of waves into the ground, we can mention the angle of refraction, the type of polarization, the transmission coefficient, and the electromagnetic properties of the ground such as the electrical permittivity[18]. In the case of parallel polarization, the transmission coefficient is obtained from equation (6), where the refraction angle is replaced by the angle of the antenna to the horizon

In this case, the sizes of the cross-sectional area of the antenna footprint in subthe surface are given by equations (7-9). In these equations $A_{TF(m)}$ are the semi-major ax and $B_{TF(m)}$ the semi-minor of the elliptical illumination on the surface.is the illuminated subsurface area in the ground. $S_{TF(m^2)}$

$$A_{TF\_v(m)} = \frac{2(H_R + \dfrac{2H_T \sin\beta}{\cos\varphi_2 + \sqrt{\varepsilon_r}\,\sin\beta})\sin\beta}{\alpha}\tan(\frac{\theta_{Az}}{2}) \tag{7}$$

$$B_{TF\_v(m)} = \frac{2(H_R + \dfrac{2H_T \sin\beta}{\cos\varphi_2 + \sqrt{\varepsilon_r}\,\sin\beta})}{\alpha}\tan(\frac{\theta_{El}}{2}) \tag{8}$$

$$S_{TF\_v(m^2)} = \frac{\pi(2(H_R + \dfrac{2H_T \sin\beta}{\cos\varphi_2 + \sqrt{\varepsilon_r}\,\sin\beta}))^2 \sin\beta}{\alpha^2}\tan(\frac{\theta_{Az}}{2})\tan(\frac{\theta_{El}}{2}) \tag{9}$$

Now, if it is perpendicular polarization, then the transmission coefficient is obtained from equation (10). In this case, the sizes of the cross-sectional area of the antenna footprint in the subsurface are given by equations (10-13).

$$\tau_h = \frac{2\eta_2 \cos\varphi_1}{\eta_2 \cos\varphi_1 + \eta_1 \cos\varphi_2} \Rightarrow \tau_h = \frac{2\sin\beta}{\sin\beta + \sqrt{\varepsilon_r}\,\cos\varphi_2} \tag{10}$$

$$A_{TF\_h(m)} = \frac{2(H_R + \dfrac{2H_T \sin\beta}{\sin\beta + \sqrt{\varepsilon_r}\,\cos\varphi_2})\sin\beta}{\alpha}\tan(\frac{\theta_{Az}}{2})$$

$$\tag{11}$$

$$B_{TF\_h(m)} = \frac{2(H_R + \dfrac{2H_T \sin\beta}{\sin\beta + \sqrt{\varepsilon_r}\,\cos\varphi_2})}{\alpha}\tan(\frac{\theta_{El}}{2}) \tag{12}$$

$$S_{TF\_h(m^2)} = \frac{\pi(2(H_R + \dfrac{2H_T \sin\beta}{\sin\beta + \sqrt{\varepsilon_r}\,\cos\varphi_2}))^2 \sin\beta}{\alpha^2}\tan(\frac{\theta_{Az}}{2})\tan(\frac{\theta_{El}}{2}) \tag{13}$$
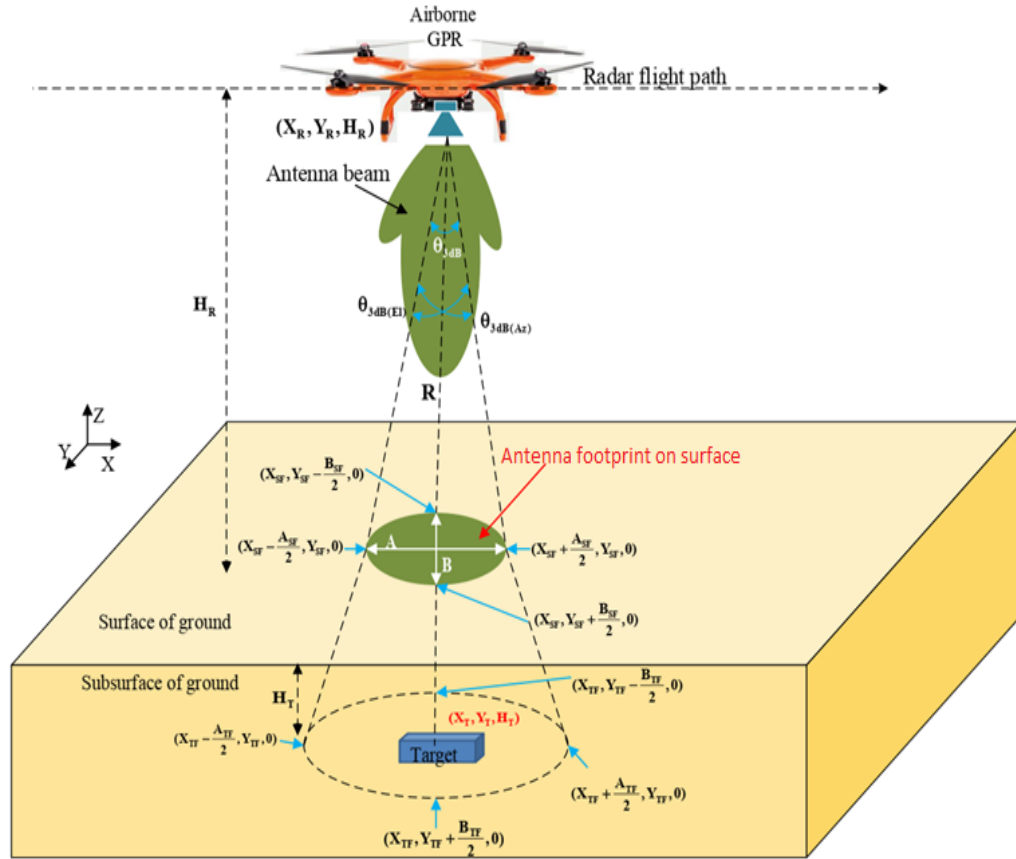
Fig. 3. The illuminated area by the antenna on the surface and subsurface in this case

a)   *Antenna footprint on the surface*

The sizes of the cross-sectional area of the antenna footprint on the surface are given by equations (14-16).

$$A_{SF(m)} = \frac{2H_R}{\alpha} \tan(\frac{\theta_{Az}}{2})$$ (14)

$$B_{SF(m)} = \frac{2H_R}{\alpha} \tan(\frac{\theta_{El}}{2})$$

$$(15)\, S_{SF(m^2)} = \frac{\pi(2H_R)^2}{\alpha^2} \tan(\frac{\theta_{Az}}{2}) \tan(\frac{\theta_{El}}{2})$$ (16)

a)   *Antenna footprint in the ground's subsurface*

In this case, the transmission coefficient is independent of the polarization, so the sizes of the cross-sectional area of the antenna footprint in the subsurface are given by equations (17-19).

$$A_{TF(m)} = \frac{2(H_R + \frac{2H_T}{\sqrt{\varepsilon_r}})}{\alpha} \tan(\frac{\theta_{Az}}{2})$$ (17)

$$B_{TF(m)} = \frac{2(H_R + \frac{2H_T}{\sqrt{\varepsilon_r}})}{\alpha} \tan(\frac{\theta_{El}}{2})$$ (18)

$$S_{TF(m^2)} = \frac{\pi(2(H_R + \frac{2H_T}{\sqrt{\varepsilon_r}}))^2}{\alpha^2} \tan(\frac{\theta_{Az}}{2}) \tan(\frac{\theta_{El}}{2})$$ (19)

III. SIMULATION OF AN AIRBORNE MONOPULSE GPR PERPENDICULAR TO THE GROUND

One of the important methods for the detection of buried targets by airborne GPR is measuring the traveled time of the electromagnetic wave from the moment it is sent by the transmitter antenna until it hits the target and is backscattered to the receiver antenna. Travel time also corresponds to the radar range, since the velocity of electromagnetic waves is the relative constitutional permittivity of the propagation medium. Propagation velocity decreases with increasing relative permittivity. The depth of the placing target $(d_{T(m)})$ is calculated by recording the elapsed time (Δt) between transmission and reception of reflections and considering the velocity of the electromagnetic wave in propagated environments according to the (20)[3, 20]

$$d_{T(m)} = \frac{C}{2 \times \sqrt{\varepsilon_r}} \times \Delta t$$ (20)

NOTE: In airborne GPR, the radar transmitter and receiver are located in free space. The target is generally located in the ground's sub-surface; the velocity of electromagnetic waves in these two environments is different, which should be considered in equation (20).

To simulate the detection of buried targets by an airborne GPR, the time signal radar part of CST software has been used. The simulation consists of three phases. In the first phase, a monostatic airborne GPR is simulated using a horn antenna as a source of electromagnetic wave propagation. In the second phase, a simulation has been made using the antenna footprint on the surface's ground, taking into account the propagation and position parameters of the antenna. In the third phase, the advantage of using the antenna footprint instead of using a radiating plate with large dimensions is stated.
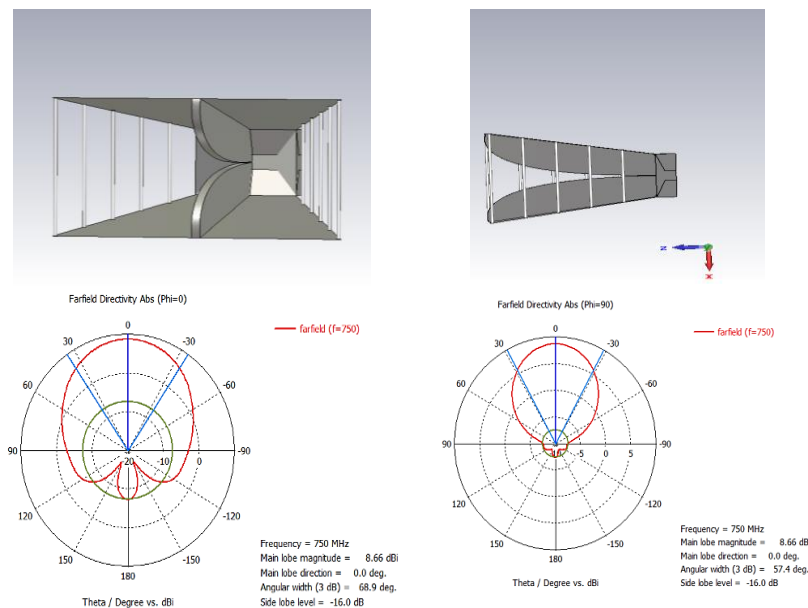
Fig. 4. The schematic of the antenna and its radiation patterns in two planes (E-plane and H-plane) at 750 MHz

A   The first phase: Simulation of a monostatic airborne GPR with an antenna for detecting buried targets

This simulation consists of three parts: antenna, ground box, and target. The antenna, as a radiation element, is responsible for sending and receiving radar signals. The field box is an environment that contains the target in itself. The target responds to the waves sent by the radar transmitter. In ultra-wideband (UWB) radars[21], the antenna must work in a wide frequency band; its broadband allows the radar to work over a large range of frequencies without changing antennas [22]. In this simulation scenario, a dual-ridged horn antenna is used, which is designed in the frequency band of 500 to 1000 MHz. Fig. 4 shows the schematic of the antenna and its radiation patterns in two planes (E-plane and H-plane) at the central frequency The azimuth and elevation half-power beam width are respectively 68.9 and 57.4 degrees. The distance between the antenna and the ground box is 3 meters, which indicates the height of the radar. The dimensions of the ground box are meters, which is a square cube. A PEC plate is used as a target, which is placed on the floor of the ground box. A radar pulse is sent from the transmitter antenna to the ground box Fig. 5 shows the view of the first phase of the simulation and received echoes. The first echo in the diagram of Fig. 5 corresponds to the antenna output pulse. The second echo is caused by the reflection from the surface of the ground box , according to relation number 20, so by having the first delay time and considering the two-way travel time and the velocity of the wave in free space, we can calculate the distance between the radiation port and the surface of the ground box . The third echo in the received signal is caused by the reflection of the target , which determines the depth of the target by considering the time delay and taking into account the two-way travel time   and the velocity of the wave in the environment (commensurate with the relative permittivity).
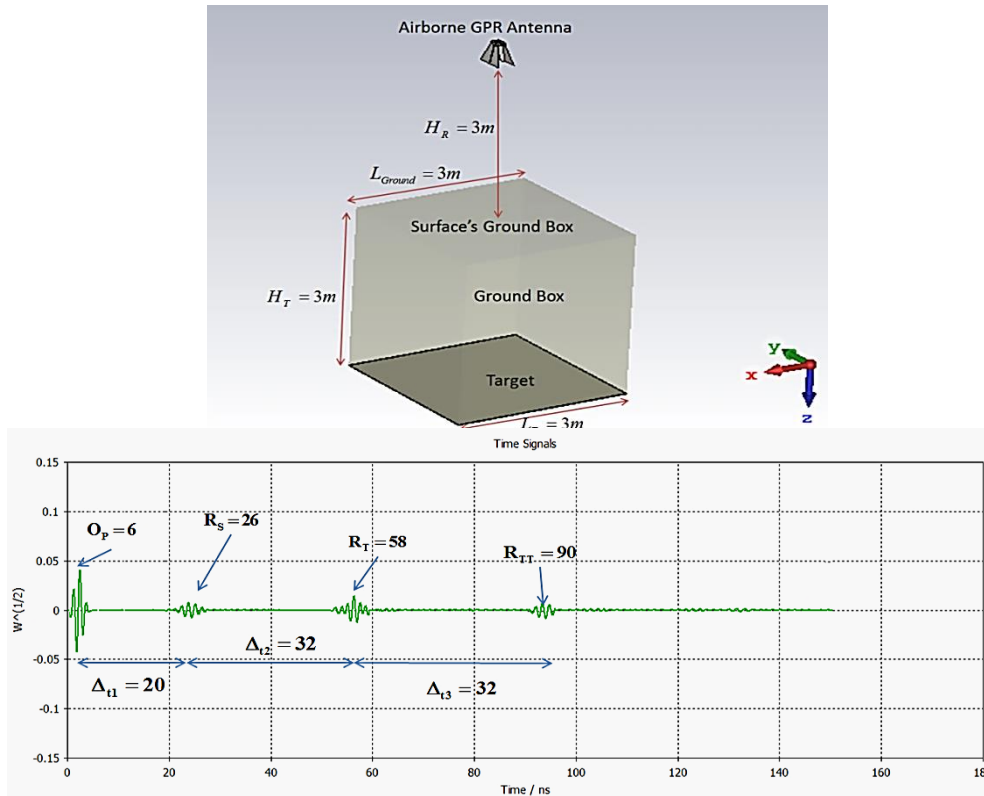
Fig. 5. The view of the first phase simulation and receiving echoes

The fourth echo in the received signal is caused by the double reflection of the target (R_{TT}).

The two-way travel time in this section is equal to the previous section $(\Delta_{t3} = \Delta_{t2})$ of the target (R_{TT}). The two-way travel time in this section is equal to the previous section $(\Delta_{t3} = \Delta_{t2})$.

$$d_{Antenna\_Surface(m)} = \frac{C}{2 \times \sqrt{\varepsilon_r}} \times \Delta t = (\frac{3 \times 10^8}{2 \times \sqrt{1}})(20 \times 10^{-9}) = 3m$$

$$d_{Surface\_Target(m)} = \frac{C}{2 \times \sqrt{\varepsilon_r}} \times \Delta t = (\frac{3 \times 10^8}{2 \times \sqrt{2.53}})(32 \times 10^{-9}) = 3.017m$$

B.   *The second phase: Simulation of detecting buried targets by using the airborne GPR antenna footprint on the surface*

In the second phase of the simulation, instead of using the antenna, we use its radiation parameters to calculate the footprint on the surface of the ground box. The dimensions of the ground box and the target are the same as in the previous phase of the simulation. The sizes of the cross-sectional area of the antenna footprint on the surface are given by equations (13-14). According to these equations, is the semi-major ax and is the semi-minor of the elliptical illumination on the surface. Fig. 6 shows the view of the second phase of the simulation and received echoes. The first echo in the diagram of Fig. 6 corresponds to the radiation port . The second echo in the received signal is caused by the reflection
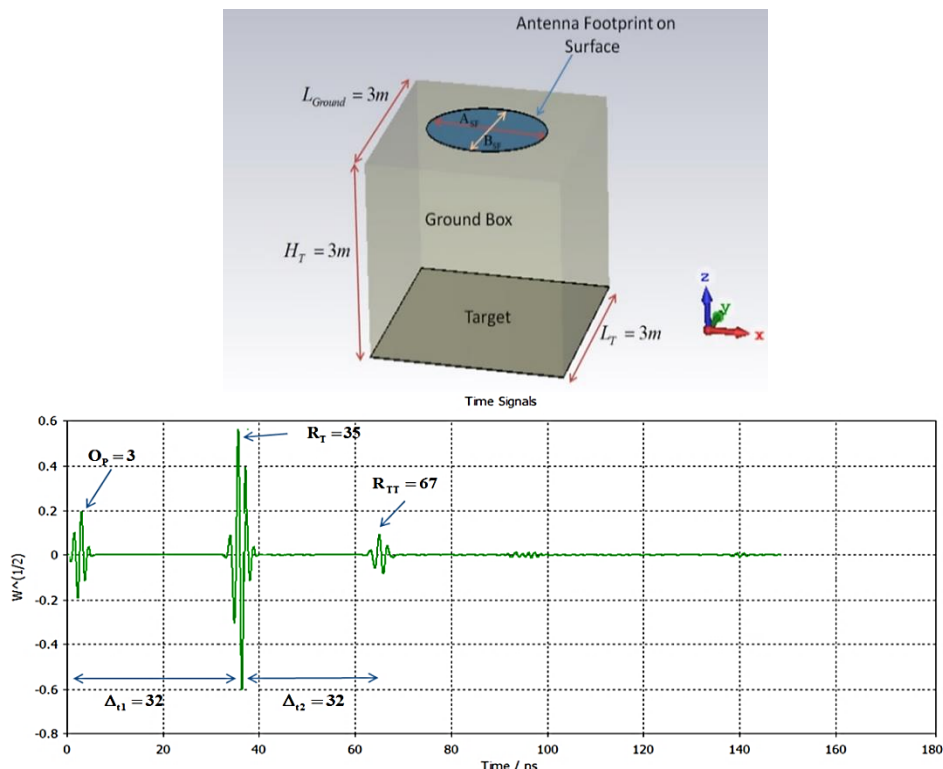
Fig. 6. The view of the second phase simulation and receiving echoes

of the target (R_T) and the third echo in the received signal is caused by the double reflection of the target (R_{TT}).

1) Comparison of the results obtained in both simulation phases

To compare the results of the first and second phases, their output signals are shown in Fig. 7. In the first phase of the simulation, a part of the signal path is in free space, which causes a sharp decrease in the signal amplitude, so we have increased its amplitude by 10 times to better display the signal related to the first phase. According to the obtained results, if we simulate the height of the antenna in the second phase and consider its equivalent as a delay parameter, the responses will match exactly. So, with this solution, the complexity of simulating the airborne GPR can be reduced to a great extent. Table I gives the number of simulation mesh cells using an antenna or footprint. Due to the drastic reduction in the number of mesh cells, if we use the antenna footprint, the simulation time is greatly reduced.

C. The third phase: The simulation of using the antenna footprint for detecting the small targets that are close to each other

Another advantage of using a radiation plane to the size of the antenna footprint is the detection of small targets that are close to each other. In this case, when the radiation port is placed above any target, that target will be revealed. To demonstrate this application, a scenario was simulated for
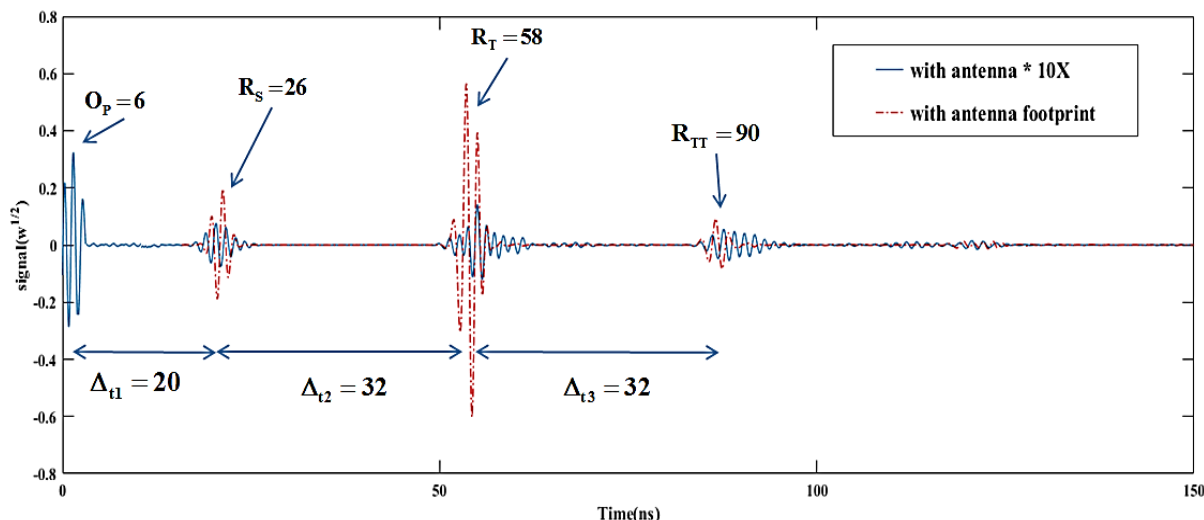
Fig. 7. The comparison of results in the first and second simulation phases

TABLE I. The number of simulation mesh cells using antenna or footprint in CST software

Airborne GPR simulation	Frequency (MHz)	AZ_HPBW (degrees)	EL_HPBW (degrees)	Semi-major - ax (m)	Semi-minor - ax (m)	Mesh cells
With antenna	500	91.8	66.2	-	-	23550120
	750	68.9	57.4	-	-	
	1000	66.4	62.1	-	-	
With footprint	500	91.8	66.2	2.08	1.31	2822960
	750	68.9	57.4	1.38	1.1	2863288
	1000	66.4	62.1	1.32	1.21	2883426

detecting two conductive plates with dimensions of a meter as a target in CST software. The dimensions of the ground box have been considered for this stage of the simulation to be metered so that we can place two targets at a suitable distance from each other. The first target is placed on the floor of the box and the second target is placed at a higher height than the first target by the length of the target.

1) The simulation of using the radiation plane with dimensions of the surface ground box

In the first stage of this scenario, a radiation plane with dimensions of the surface of the ground box as a radiation port is used. The outline of this stage of simulation and its output diagram are shown in Fig. 8. According to the obtained results, not be able to identify two targets from each other, and in the simulation output, two targets were seen at once. According to relation number 20 and obtained the first delay time, concluded that the depth of placement of targets also had an error.
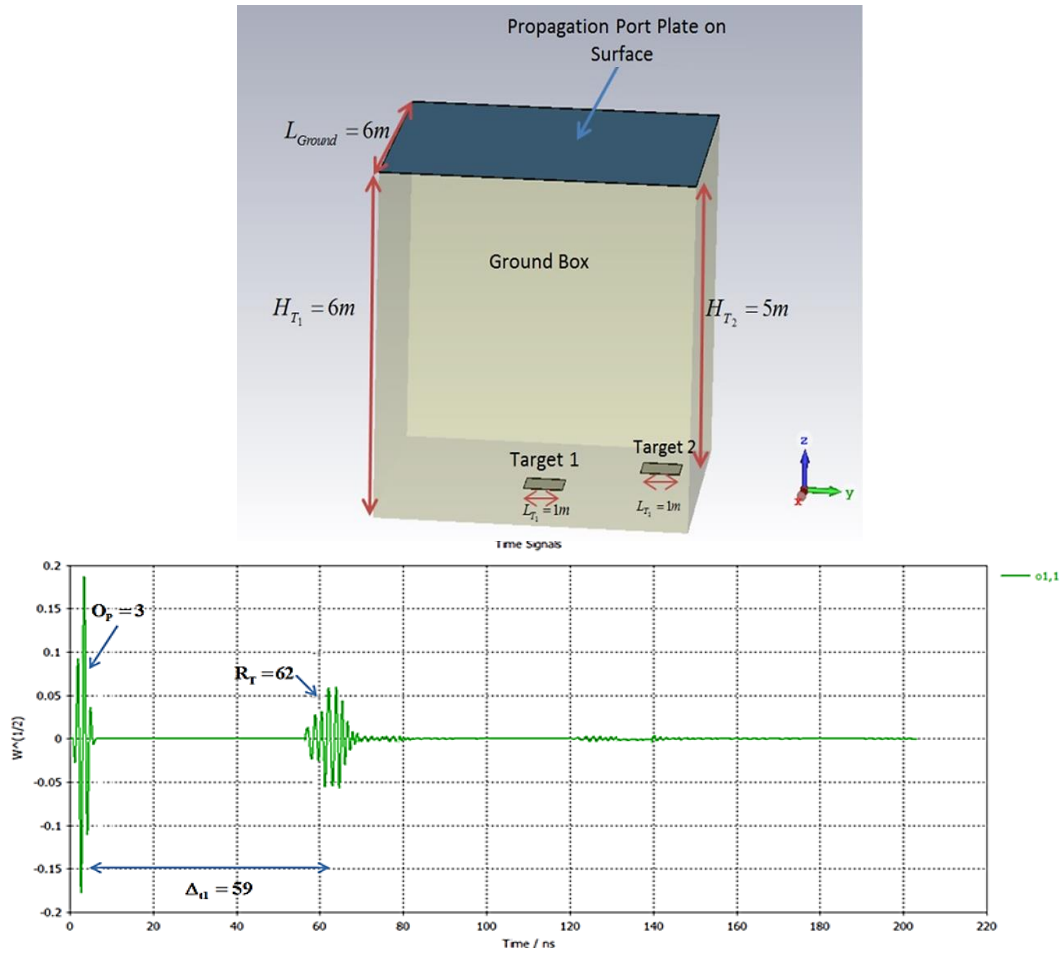
Fig. 8. The simulation of using the radiation plane with dimensions of the surface ground box and receiving echoes

$$d_{Surface\_Target(m)} = \frac{C}{2 \times \sqrt{\varepsilon_r}} \times \Delta t = (\frac{3 \times 10^8}{2 \times \sqrt{2.53}})(59 \times 10^{-9}) = 5.563m$$

2)   The simulation of using the antenna footprint in the center of the surface ground box

In the second step, the antenna footprint corresponding to the dimensions of the previous phase is used as the radiation port and is placed exactly in the center of the surface of the ground box above the first target. At this stage, when the antenna footprint is in the center of the surface, the first target located on the floor of the box will be identifiable. The outline of this stage of simulation and its output diagram are shown in Fig. 9 and according to relation number 20 and the obtained time delay, concluded that the depth of placement of the first target has been achieved almost correctly.

$$d_{Surface\_Target_1(m)} = \frac{C}{2 \times \sqrt{\varepsilon_r}} \times \Delta t = (\frac{3 \times 10^8}{2 \times \sqrt{2.53}})(63 \times 10^{-9}) = 5.941m$$
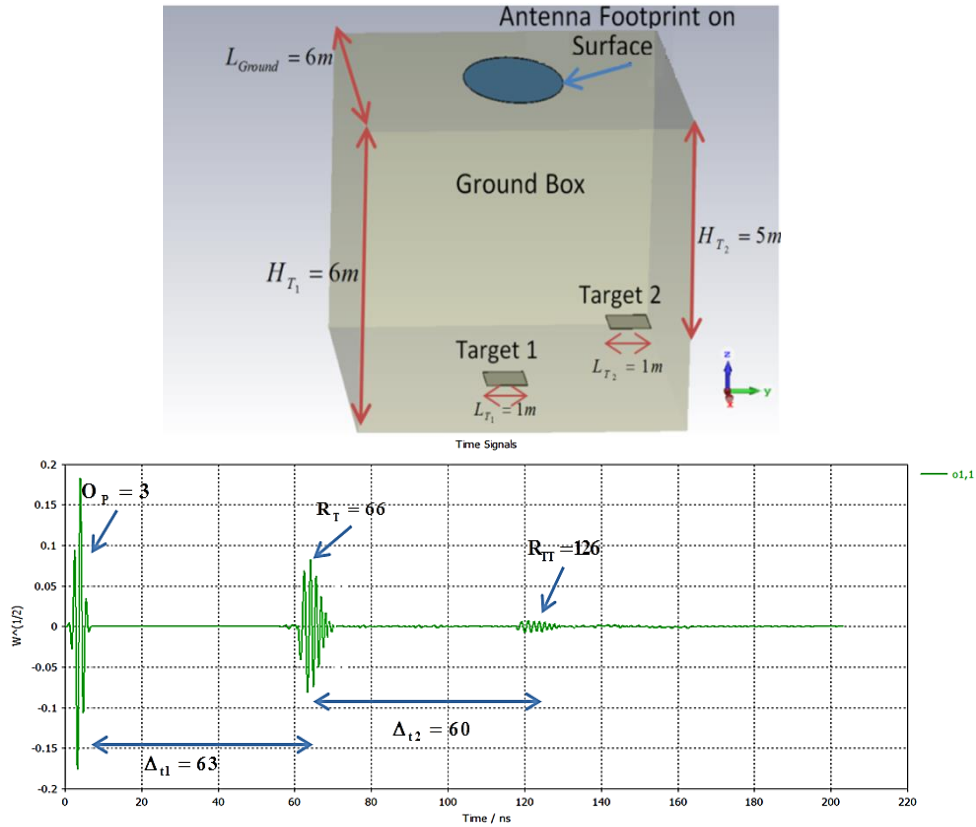
Fig. 9. The simulation of using the antenna footprint on the center of the surface ground box and receiving echoes

3) The simulation of using the antenna footprint on the side of the surface ground box

In the third step of the simulation, the footprint of the antenna moved to the top of the second target and on the surface of the soil box. In this instance, it is anticipated that the second target will be uncovered. it is located at a higher height than the first target. The figure shows this simulation stage and its output diagram in Fig. 10. According to the obtained time delay and the relation number 20, concluded that the depth of the second target was also obtained almost correctly.

$$d_{Surface\_Target_2(m)} = \frac{C}{2 \times \sqrt{\varepsilon_r}} \times \Delta t = (\frac{3 \times 10^8}{2 \times \sqrt{2.53}})(53 \times 10^{-9}) = 4.998m$$

According to the obtained results and simulations, it can be concluded that the use of antenna traces can be effective in detecting and identifying small targets close to each other. These targets cannot be recognized by the radiation wave plate larger than the footprint of the antenna; they can be separated only if they are far enough apart in terms of placement height.
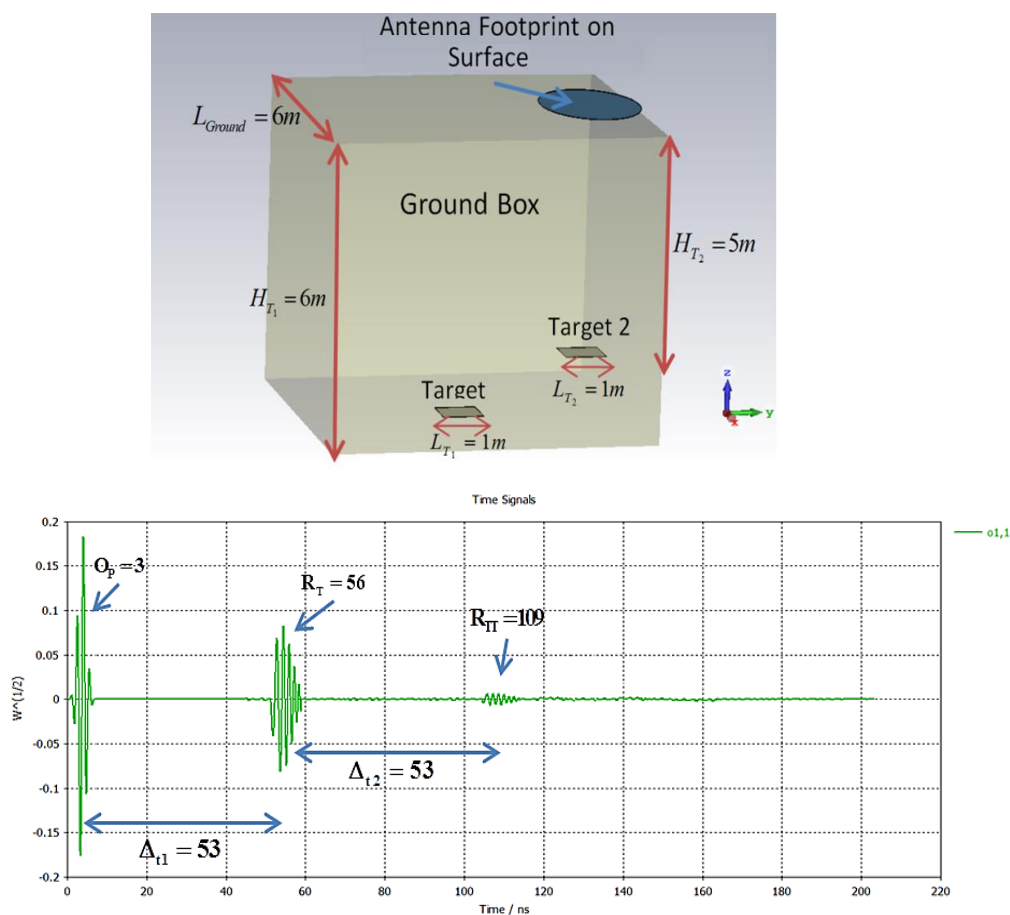
Fig. 10. The simulation of using the antenna footprint on the side of the surface of the ground box and receiving echoes

IV. CONCLU

V. SIONS

In the topic of detecting buried targets by airborne GPR radars, knowing the area illuminated by the radar antenna is very important. The effective factors in determining the dimensions of the illuminated area on the surface are the position of the radar antenna, the azimuth and elevation half-power beam width, and on the ground's subsurface, in addition to the above-mentioned parameters, the relative permittivity of the ground and the height of the desired area to surface, the type of polarization and the refraction angle of the waves sent from the radar are dependent. In this paper, all the dependences of the illuminated ground's subsurface are generalized to the characteristics of the transmitter antenna and the transmitted wave, and we can calculate its dimensions only by knowing the relative permittivity of the ground. By having the dimensions of the illuminated area, we can cell the search area according to it and excite these cells with appropriate power and at a certain time. The advantages of cell confinement according to the antenna footprint are managing the transmitted power and reducing the search time. In this paper, two methods are provided to simulate the detection of

buried targets in CST software. In the first method, a horn antenna is used as a radiation element in the structure itself, but in the second method, the antenna is simulated separately and its parameters are used to calculate the antenna footprint. In the first method, the meshing is very large due to the distance between the antenna and surface, which increases the simulation time, but in the second method, due to the removal of this distance and the use of the antenna footprint as a radiation element, the meshing And the simulation time is greatly reduced. In the second method, we include the amount of signal delay that is proportional to the height of the antenna as a correction parameter in the outputs, in which case both simulations will have almost the same results. Another advantage of using a radiation plane to the size of the antenna footprint is the detection of small targets that are close to each other. In this case, when the radiation port is placed above any target, that target will be revealed.

REFERENCES

[1]. F. Soldovieri and R. Solimene, "Ground Penetrating Radar Subsurface Imaging of Buried Objects," Radar Technology. InTech, Jan. 2010.

[2]. M. I. Skolnik, "Radar Handbook, Third Edition," McGraw-Hill Education, 2008.

[3]. A. S. Turk, K. A. Hocaoglu, and A. A. Vertiy, "Subthe surface Sensing," Wiley, 2011.

[4]. M. García-Fernández *et al.*, "Synthetic Aperture Radar Imaging System for Landmine Detection Using a Ground Penetrating Radar on Board a Unmanned Aerial Vehicle," *IEEE Access*, vol. 6, pp. 45100–45112, 2018.

[5]. M. R.. Castellazzi, P. Gloaguen, E. Trépanier, L. and J.Garfias, "ERT, GPR, InSAR, and tracer tests to characterize karst aquifer systems under urban areas: The case of Quebec City," vol. 310, pp. 45–56, 2018.

[6]. Z. Minxue, "Application of InSAR and GIS techniques to ground subsidence assessment in the Nobi Plain, Central Japan," *Sensors (Basel, Switzerland)* vol. 14, pp. 492-509, Dec. 2013.

[7]. B. Andrea and L. Pajewski, "Civil engineering applications of ground penetrating radar," Springer, 2015.

[8]. C. K. N. Hailma, A. Joret, M. Razali, A. Ponniran, M. S. Sulong, and R. Omar, "Frequency-based signal processing technique for pulse modulation ground penetrating radar system," *Signal Processing*, vol. 11, pp. 4104–4112, Oct. 2021.

[9]. A. Joret, M. F. L. Abdullah, and M. S. Sulong, "Simulation of GPR system design using cst microwave and MATLAB," *Yanbu Journal of Engineering and Science*, vol. 14, May 2021.

[10]. A. Joret, M. F. L. Abdullah, S. H. Dahlan, A. Madun, and M. S. Sulong, "Development of Ground Penetrating Radar Hybrid System Using Vivaldi Antenna for Buried Object Detection," *IJEEAS*, vol. 1, no. 1, pp. 39–44, Apr. 2018.

[11]. A. Joret, M. S. Sulong, M. F. L. Abdullah, A. Madun, and S. H. Dahlan, "Design and Simulation of Horn Antenna Using CST Software for GPR System," *J Phys Conf Ser*, vol. 995, no. 1, p. 1280, Apr. 2018.

[12]. M. García-Fernández *et al.*, "UAV-mounted GPR for NDT applications," *2018 15th European Radar Conference (EuRAD)*, pp. 2–5, 2018.

[13]. H. Liu *et al.*, "Detection of Cavities In Urban Cities by 3D Ground Penetrating Radar," *Geophysics*, pp. 1–44, Jan. 2021.

[14]. X. Lucas Travassos and M. F. Pantoja, "Ground Penetrating Radar," in *Handbook of Advanced Nondestructive Evaluation*, N. Ida and N. Meyendorf, Eds., Cham: Springer International Publishing, 2019.

[15]. H. M. Jol, "Ground Penetrating Radar Theory and Applications," Elsevier Science, 2008.

[16]. D. J. Daniels, "Ground Penetrating Radar (2nd Edition)," Institution of Engineering and Technology, 2004.

[17]. D. Edemsky, A. Popov, I. Prokopovich, and V. Garbatsevich, "Airborne Ground Penetrating Radar, Field Test," *Remote Sensing*, vol. 13, no. 4, p. 667, Feb. 2021.

[18]. F. T. Ulaby, D. G. Long, and A. Fung, "Microwave radar and radiometric remote sensing," Artech, 2015.

[19]. A. K. Maini, "Military Radars," in *Handbook of Defence Electronics and Optronics*, pp. 203–294, 2018.

[20]. H. Zadhoush and A. Giannopoulos, "Optimizing GPR time-zero adjustment and two-way travel time wavelet measurements using a realistic three-dimensional numerical model," *Near The surface Geophysics*, vol. 20, no. 2, pp. 208–226, Apr. 2022.

[21]. M. Garcia-Fernandez, Y. Alvarez-Lopez, and F. Las Heras, "Autonomous Airborne 3D SAR Imaging System for Subthe surface Sensing: UWB-GPR on Board a UAV for Landmine and IED Detection," Remote Sensing, vol. 11, no. 20, p. 2357, Oct. 2019.

[22]. A. R. Mallahzadeh and A. Imani, "Double-Ridged Antenna for Wideband Applications," Progress In Electromagnetics Research, vol. 91, pp.273-285, 2009.